RSC Advances




ROYAL SOCIETY OF CHEMISTRY

www.rsc.org/advances

Journal Name

RSCPublishing

ARTICLE

# Application of surface complexation modeling on modification of hematite surface with cobalt cocatalysts: a potential tool for preparing homogeneously distributed catalysts

Cite this: DOI: 10.1039/x0xx00000x

Received 00th January 2012,
Accepted 00th January 2012

DOI: 10.1039/x0xx00000x

www.rsc.org/

TsingHai Wang,[a*] Hsin-Ting Hung,[a] Wei Wang,[b] Po-Chieh Li,[c] Yi-Kong Hsieh,[a] Yingchao Dong,[d] Chu-Fang Wang,[a*]

The knowledge required to synthesize homogeneously distributed catalysts on the support surfaces is strongly relied on understanding the interaction between the catalyst and surface of support, which is identical to the descriptions of interactions between environmental pollutants and adsorbents in the field of environmental chemistry. The connection between catalyst synthesis and environmental chemistry is demonstrated herein by using surface complexation modeling (SCM), whose physical foundation is built on the stoichiometric reaction between one solute and one adsorption site on the surface of adsorbents. As suggested by our simulation and supported by TEM images, the manipulation of either homogeneous distribution or coarse clusters of cobalt cocatalysts over hematite surfaces can be achieved by adjusting the pH and initial $Co^{2+}$ concentration. This is attributed to the conversion of adsorbed $Co^{2+}$ or $Co(OH)_2$ precipitates on hematite surfaces. Different surface distributions of cobalt cocatalysts further influence the reactivity of photodegradation of organic dyes and photoelectrochemical reactions, which is strongly dependent on the occurrence of the Fenton reactions or charge transport. Our results not only demonstrate the potential of SCM on guiding the preparation of homogeneously distributed catalysts but also indicate that the abundant amount of knowledge in the environmental science could be adopted to design an appropriate protocol for catalyst synthesis.

*KEYWORDS: surface complexation modeling; homogeneously distributed catalyst; photoelectrochemical cell; photodegradation; hematite*

## Introduction

The idea of single-atom catalysts (SACs) is to greatly enhance the utilization efficiency of noble metals on support surfaces.[1] In comparison with nanoparticles and clusters, the surface free energy of SACs was maximized and stabilized via the formation of metal-O-support bindings.[2,3] Several methods have been proposed to prepare SACs, including impregnation or ion-exchange techniques, coprecipitation, colloidal deposition method, templates, and adsorption of metal complexes followed by thermal treatment.[4] Among them, the last one has been widely adopted as a major route to prepare SACs due to the simplicity of preparation. However this preparation route strongly relies on the knowledge regarding to the interaction between metal complexes and support surface, which leads to limited success in the literature. Despite the following thermal treatment is another important factor as it often invariably leads to a variety of mixed oxides, knowledge to manipulate homogeneously distributed metal complexes over support surfaces is highly desired in the first place. Although the relevance may not sound obviously, this issue actually shares remarkable similarities with the one of the most important research topics in the environment science community- understanding the mechanism of pollutant immobilization by adsorbents such as clay, zeolite, iron oxides and others, which also involves the interaction between metal complexes and adsorbents. In these cases, surface complexation modeling (SCM) have been successfully applied to simulate and explain the interactions between adsorbent surfaces and metal complexes of concern.[5-7] The physical basis of SCM is built on the stoichiometric adsorption reaction between one surface adsorption site and one metal complex/ion driven by electrostatic interaction in a manner consistent with mass and charge balances.[8,9]

Taking hematite ($Fe_2O_3$) as an example, it is one of the most important nature occurring minerals regulating the transport of pollutants in aquifer and soil. Hematite is also known as a promising

photocatalyst, whose widespread application is currently limited by the slow water oxidation kinetics. By associating with a few weight percentage of cobalt-based cocatalyst, its photocatalytic performance is demonstrated greatly improved as a result of the reduction in the recombination losses and thus more photogenerated holes are able to participate in water oxidation.[10-13] Several methods were proposed to associate cobalt cocatalyst onto hematite surface, including atomic layer deposition (ALD),[14] (photo)electrodeposition,[13,15-18] thermal hydrolysis,[10-12] and post treatment.[19] These preparation methods, except ALD and thermal hydrolysis, are conducted in a solution containing different concentrations of $Co^{2+}$, sometimes along with some structure directing agents. Despite their success in producing efficient hematite photoelectrodes, our preliminary SCM simulation suggests that the surface of hematite on photoelectrodes cannot accommodate such a large amount of Co-cocatalysts if they were associated by adsorption reaction. For example, the maximum surface adsorption site density based on crystallographic calculation of surface hydroxyl configuration of hematite was determined to be 7.5 sites/nm$^2$.[20] Taking the most widely studied hematite photoelectrode with a working area of 1 cm$^2$ as an example, the maximum number of $Co^{2+}$ adsorbed on this surface would be no greater than $7.5 \times 10^{14}$ (~ 1.25 nmole, assuming a nonporous surface). This value is obviously several orders of magnitude smaller than any reported values (a few weight percent) in the literature. This simulation apparently conflicts with the observations where a thin $Co_3O_4$ layer (~ tens to hundreds nm thickness) is found on the top of hematite layer in these successful cases. In this configuration, the photogenerated holes that participate in water oxidation at $Co_3O_4$ /water interface are actually those that have to transport through additional thousands of grain (or grain boundary) of in the $Co_3O_4$ layer. This also reflects the fact that the knowledge regarding to the hematite/Co interface phenomenon is not yet fully understood. Accordingly, an effective method to prepare homogeneously distributed $Co_3O_4$ over the surface of hematite is highly desired to fulfill the need for the future exploration in hematite/Co interface phenomenon.

In this study, we demonstrate the application of SCM as guidance to manipulate the distribution of $Co_3O_4$ on hematite surface. This is possible, as described previously, because the physical foundation of surface complexation modeling is built on the stoichiometric reaction between the solutes and adsorbent surfaces as shown in Eqn (1),

$$SOH + Co^{2+} \leftrightarrow SOCo^{+} + H^{+}, \qquad \text{Eqn (1)}$$

where S refers to the adsorption site on hematite surfaces.[8,7,21] Also, a detail discussion toward the mechanism behind those successfully synthesizing high efficiency cobalt decorated hematite electrodes is given from the point of view of surface chemistry. An illustration of the configuration of SCM is shown in the Scheme 1 in the supporting material.

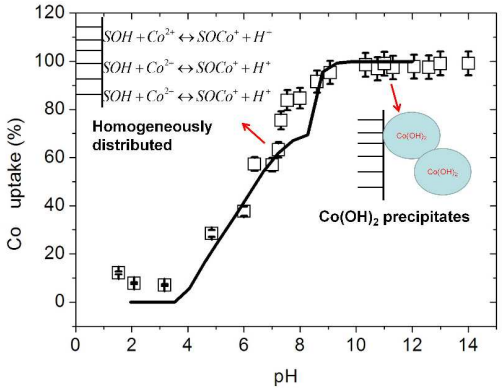


**Scheme 1**. The illustration of how surface complexation modeling can be applied to design an appropriate synthesis protocol to manipulate the distribution of Co cocatalysts on hematite surfaces.

## Experimental

All chemicals were ACS grade and deionized water was used throughout all experiments. For hematite nanoparticle synthesis, two liters 20 mM $FeCl_3$ aqueous solution was sealed in a serum bottle and aged at 100 $^oC$ for 2 days.[22] Cobalt adsorption experiments were conducted in triplicate by mixing 1.0 ~ 10 g hematite with 100 mL 10 ~ 0.01 mM $Co^{2+}$ solutions (prepared by dissolving aliquot amount of $Co(NO_3)_2 \cdot 6H_2O$, Sigma-Aldrich) under different pH environments. In the end of 24 hours of adsorption, the mixtures were centrifuged and the concentrations of $Co^{2+}$ remaining in supernatants were determined by ICP-MS (7500a ICP-MS, Agilent). The difference in the $Co^{2+}$ concentration in the supernatant was assumed the amount of Co adsorbed/precipitated onto hematite surfaces. Detailed experimental conditions of each sample are listed in Table S1. On the other hand, the centrifuged mixtures were first dried at 60 $^oC$ and then subjected a two-step calcination treatment (500 $^oC$ 2 hours and then 700 $^oC$ 20 minutes) and stored under ambient environment before further photocatalytic experiments. The water chemistry and SCM simulation were conducted using MINEQL, an aqueous chemical equilibrium calculation software. Several assumptions were made prior to SCM simulations in order to keep the number of adjustable parameters as low as possible. First, the surface adsorption site density was assumed to be 7.5 sites/ nm$^2$.[20] Given that $Co^{2+}$ adsorption experiments were conducted with a solid/liquid ratio of 1.0 g hematite/100 mL solution, the corresponding adsorption site concentration in the system was 0.71 mmol/L (the surface area of hematite particles determined by $N_2$-BET method is 8.47 m$^2$/g). Second, as the equilibrium constant is a state function, we adopted the logKa1 as 6.9 for protonation reaction and logKa2 as -12.8 for the deprotonation reaction of hematite, respectively (Eqn (2) and (3)).[7] Last, we assumed the hematite surface is homogeneous, although it is suggested that there are roughly 2 % of the surface adsorption sites belonging to the strong sorption sites.[21]

$$SOH + H^{+} \leftrightarrow SOH_2^{+} \qquad \text{Eqn (2)}$$

$$SOH \leftrightarrow SO^{-} + H^{+} \qquad \text{Eqn (3)}$$

The photocatalytic activity of as-obtained cobalt-loaded hematite samples was evaluated by both rhodamine B (RhB) dye photodegradation (conducted in pH 7.2 ± 0.2) and by water splitting reaction (1.0 M NaOH solution, pH = 13.6) under the illumination of 100 mW/cm$^2$ simulated sunlight (AM 1.5G). For RhB photodegradation experiments, 0.02 g of hematite samples were dispersed in 100 mL of solution containing 0.02 mM RhB and 50 mM $H_2O_2$.[26] The assembly of cobalt-loaded samples onto FTO substrates was conducted following by our previous proposed DA method.[29] All photoelectrochemical measurements including impedance spectroscopy were conducted using a three-electrode configuration: a hematite photoanode as the working electrode, a saturated calomel electrode (SCE) as the reference electrode, and platinum foil as the counter electrode in 1 M NaOH and a CH Instrument 604E electrochemical workstation under 100 mW/cm$^2$ illumination. Obtained data was fitted by an equivalent circuit model using Zview software.

**Results and Discussion**

We first conducted a series of $Co^{2+}$ adsorption experiments with synthesized hematite nanoparticles and fitted as-obtained experimental sets with SCM to determine the adsorption equilibrium constant.

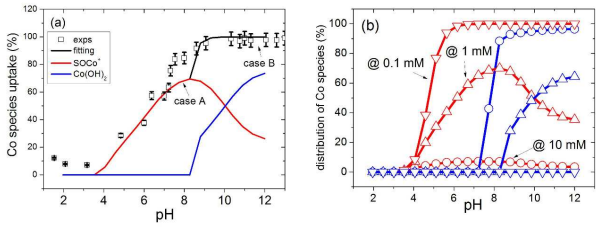


**Figure 1.** (a) Result of Co adsorption experiments and fitting (initial $Co^{2+}$ concentration= 1 mM; solid/liquid ratio= 1 g/ 100 mL; fitting parameters: adsorption reaction equilibrium constant pK = 1.5; red: the fraction of adsorbed $Co^{2+}$ species; blue: the fraction of $Co(OH)_2$ precipitate; black: the sum of the fraction of adsorbed $Co^{2+}$ and $Co(OH)_2$ precipitate); (b) the simulation of relative Co species distribution in different initial $Co^{2+}$ conditions; red: adsorbed $Co^{2+}$ species, blue: the fraction of $Co(OH)_2$ precipitates

Based on above assumptions, the best fitting was shown in Figure 1a, where the best fitting curve (black) is the sum of the fraction of adsorbed $Co^{2+}$ (red) and those of precipitated $Co(OH)_2$ (blue). It is worth mentioning that although the adsorption edge can be fitted nicely, the fitting curve failed to describe the adsorption behaviors at pH > 7. Specifically, the fitted adsorption plateau occurred at the region of neutral pH with a Co uptake around 0.7 (red, Figure 1a), while experimentally observed adsorption plateau was near unity. In the framework of SCM, the adsorption plateau physically means that all active adsorption sites are occupied by $Co^{2+}$ cations under equilibrium. The discrepancy between the fitting and experimental results can be explained by the formation of surface precipitation (blue, Figure 1b). The term surface precipitation is particularly standing for a phenomenon where the adsorption isotherm departs from the linearity. This is because the amount of loaded Co species obviously exceeds the adsorption capacity of hematite, leading to a solid-like precipitate of Co species over hematite surface. Indeed, the abrupt rising of $Co^{2+}$ uptake experimentally observed in Figure 1a stemmed from the formation of $Co(OH)_2$ precipitate, as confirmed by our simulation. This means that the observed $Co^{2+}$ uptake at basic pH was a result of the combination of adsorbed $Co^{2+}$ and precipitated $Co(OH)_2$ (black, Figure 1a). This is very important as the adsorption experiment only allows us to evaluate the concentration difference in the solution but cannot tell the reaction and mechanism how these Co species are removed by hematite. Additional aqueous chemistry simulations showed that the threshold concentration for cobalt ions to form $Co(OH)_2$ precipitates was around 1 mM (blue ▽, Figure 1b). Furthermore, this threshold concentration shifted to lower pH values as initial $Co^{2+}$ concentration increased (blue ○, Figure 1b). In consistent with results reported by Kobal et al.,[23] this means a high initial $Co^{2+}$ concentration is prone to induce hematite surface covered with a large number $Co(OH)_2$ precipitates.

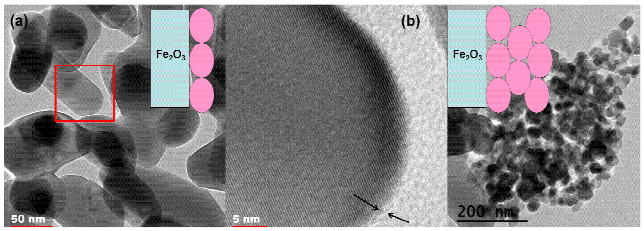


**Figure 2.** Representative TEM images and illustrations of hematite covered with (a) a monolayer of $Co_3O_4$ nanoparticle (case A in Figure 1a, barely visible), (b) high magnification image of the zone indicated in Figure 2a, and (c) with $Co_3O_4$ clusters (case B, in Figure 1a). Inserted magenta circles refer to $Co_3O_4$ cocatalysts.

The Co association to hematite surface by adsorption (case A, Figure 1a) and precipitation (case B, Figure 1b) can be visualized from TEM images as shown in Figure 2. The hematite sample prepared in a condition with 1 mM $Co^{2+}$ at pH 8 (equilibrated pH) is expected to have $Co^{2+}$ stoichiometrically adsorbing on the hematite surface without any $Co(OH)_2$ precipitate. These adsorbed $Co^{2+}$ cations were subsequently converted into fine $Co_3O_4$ nanoparticles in the end of thermal treatment (confirmed by XPS, Figure S1) that is barely observable in the TEM image (Figure 2a). Under the high magnification, a thin layer with thickness ~ 2 nm on the surface of hematite is observed (Figure 2b), indicating Co-cocatalysts prepared through the adsorption would be in favor of developing into a thin $Co_3O_4$ layer. Similar phenomenon has been reported by Deng et al., where a thin layer of carbon (~ 2 nm) on the surface of hematite was observed as a result of pyrolysis of ferrocene. This thin carbon layer further modifies the electronic structure of hematite, leading to a photocurrent about four times higher than the those without carbon layer.[25] In contrast, those obtained from the case B condition contained a large amount of visible $Co_3O_4$ clusters with size approximately in the range around 10-30 nm (Figure 2c). Again, subsequent thermal treatment may produce mixed oxides of iron and cobalt which is difficult to distinguish by the darkness in Figure 2c. However, it is certain that the coarsen $Co_3O_4$ clusters are a result of $Co(OH)_2$ precipitation while homogeneously distributed $Co_3O_4$ could be achieved through the adsorption. Based on these observations, we propose two likely scenarios of how surface $Co_3O_4$ were disperesed on hematite surfaces (inserted panels in Figure 2a and 2c). First, homogeneously distributed $Co_3O_4$ can be prepared by dispersing hematite particles in a solution with neutral pH and a low initial $Co^{2+}$ concentration, i.e., 1 mM (case A, Figure 1a) to avoid the formation of $Co(OH)_2$ precipitates. By contrast, $Co_3O_4$ clusters could be obtained by preparing samples in a solution containing high $Co^{2+}$ concentrations at high pH (case B, Figure 1a). Our speculation is substantially supported by results from following zeta potential

measurements (Figure S2). As expected, the zeta potential of hematite is pH sensitive with the point of zero charge ($pH_{pzc}$) around pH 8.8. The zeta potential of hematite with a thin layer of Co cocatalyst (case A) resembles that of hematite but its $pH_{pzc}$ is shifted to ~ pH 7.2. In contrary, the zeta potential of hematite with coarse $Co_3O_4$ clusters (case B) becomes less pH dependence, possessing a negative surface charge around -10 mV when pH exceeding pH 4.8. The reported $pH_{pzc}$ of $Co_3O_4$ using both potentiometric titration and zeta potential measurement was determined around pH 7.5,[26] which is very close to that of case A samples. This indicates that the surface chemistry of case A samples is very similar to that of $Co_3O_4$, which is a complementary evidence besides the observations from TEM image (Figure 2b). The cause of the surface chemistry of case B samples behaving pH-independent remains unclear; however, it should be closely related to the interactions between hematite and $Co_3O_4$ clusters on hematite surfaces.

Based on our results, SCM is indeed a powerful tool to design an appropriate protocol for the dispersion of $Co_3O_4$ on hematite surfaces. Also, SCM simulation allows us to understand the mechanisms regarding to how $Co_3O_4$ is associated on hematite surfaces by electrolysis[15] and photodeposition.[13,16,18,27] In these cases, the association of $Co_3O_4$ to hematite surfaces was conducted in a solution containing 1.0 M phosphate with the initial $Co^{2+}$ concentration of 0.5 mM in the neutral pH environment. Although the effect of pH on ions adsorption to the support is well known for a long time, we herein attempt the address this phenomenon from the point of view of aqueous and surface chemistry considerations based upon the SCM simulations. As demonstrated in Figure 1b, a low initial $Co^{2+}$ concentration prevents the formation of $Co(OH)_2$ precipitates, whereas a neutral pH guarantees the deprotonation of hydroxyl groups on hematite surface so that they are available for $Co^{2+}$ accommodation. This condition is in favor of producing fine $Co_3O_4$ clusters as they are known possessing high reactivity (size smaller than 5 nm).[10,27] This is very important since the charge transfer from hematite to $Co_3O_4$ clusters is much kinetically favorable when they are located inside the Helmholtz layer of the hematite surfaces.[27] In contrast, those $Co_3O_4$ loaded hematite samples prepared through the hydrothermal reaction are expected to be possessing very limited $Co_3O_4$ clusters as SCM simulations predict that cobalt adsorption to hematite in an acidic environment is thermodynamically unfavorable (Figure 1b). There may be a small population of $Co^{2+}$ allowed to be uptake by strong adsorption sites, which accounts for < 2% of total adsorption sites on hematite surfaces.[9] In this case, the amount of loaded $Co_3O_4$ would be too small to have any significant influence on photocatalytic performance enhancement. Therefore, the possible mechanism responsible for these successful studies through the hydrothermal reaction is by the consideration of the deposition of hydrolysis product of Co(OOH) on hematite surface.[11,12] In these cases, following thermal treatment transforms Co(OOH) precipitates into coarse $Co_3O_4$ clusters and thus enhanced photocatalytic activity was achieved.

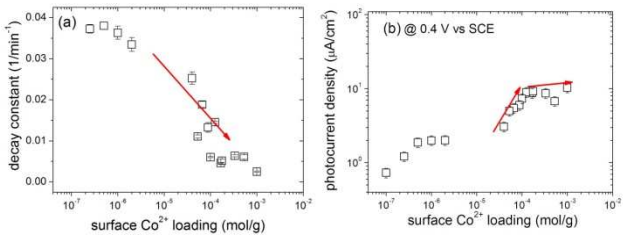


**Figure 3.** (a) determined RhB dye photodegradation constants and (b) Photocurrent density of hematite particles decorated with different cobalt cocatalysts as a function of surface cobalt cocatalyst loadings.

In order to demonstrate the effect of different distributions of surface $Co_3O_4$ on photocatalytic performance, RhB dye photodegradation and water splitting reactions were conducted under simulated sunlight illumination. Figure S3 shows the representative photodegradation profiles of RhB dye using different hematite samples. The results show that although $Co_3O_4$ is an effective catalyst in water oxidation, charge carrier transfer (photogenerated holes) is apparently not the dominant step in the photodegradation of RhB dyes. Instead, it is likely the Fenton reaction is mainly responsible for organic dye photodegradation.[28] In this case, the degradation of RhB dyes under visible light illumination is suggested following two successive stages.[29] First, dye molecules are photoexcited and the electrons transfers from the excited dye molecules to surface $Fe^{3+}$ ions, which is accompanied with reduction of $Fe^{3+}$ to $Fe^{2+}$. Reduced $Fe^{2+}$ ions then react with $H_2O_2$ to generate OH radicals which initiate the photocatalytic reaction to mineralize the organic dyes. In this sense, the higher $Co_3O_4$ loading on the surface of hematite, the less surface $Fe^{3+}$ are available to participate in the Fenton reaction. This explains the decrease in the decay constant *k* along with increasing surface $Co_3O_4$ loadings (Figure 3a). It is worth mentioning that distinguishing the influence of $Co_3O_4$ that is converted by $Co(OH)_2$ precipitates from those by adsorption is very difficult as the former always contained a significant fraction of the latter (blue symbols in Figure 1b). However, it is clear that once hematite surface is covered with $Co_3O_4$, fewer surface $Fe^{3+}$ ions are available for participating in Fenton reaction and thus slower photodegradation of RhB dye is observed.

When assembling these cobalt decorated hematite samples onto FTO substrates, we noted that the surface $Co_3O_4$ substantially improved the photocurrent density (Figure S4). In contrary to the observations noted in the case of RhB dye photodegradation, photocurrent indeed increases with increasing surface $Co_3O_4$ loadings (Figure 3b). This means charge transfer reaction is the essential step accounting for the photocurrent enhancement.[19] Importantly, the degree of photocurrent enhancement is strongly dependent on the dispersion of $Co_3O_4$ on hematite surfaces (Figure 3b). For instance, observed photocurrent increased steeply as surface $Co_3O_4$ loading increased to a level around $10^{-4}$ mol/g. This enhancement is suggested as a result of surface $Co_3O_4$ effectively retarding the electron/hole recombination.[13,17] In this way, surface $Co_3O_4$ plays as a surface state at which photogenerated holes are transferred from hematite to $Co_3O_4$ and then to the electrolyte.[30] By contrast, the photocurrent stops significantly increasing when hematite was covered with $Co_3O_4$ clusters (with surface $Co_3O_4$ loading exceeding $10^{-4}$ mol/g). Again, this is in a good agreement with literature that coarse $Co_3O_4$ is less reactive than the finer ones.[10,24]

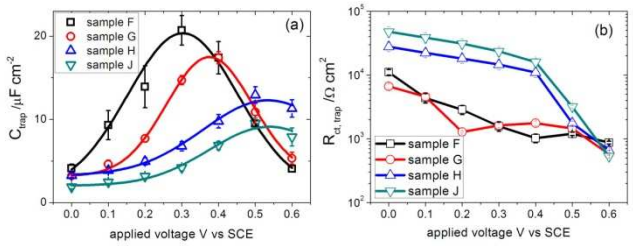


**Figure 4.** Determined (a) $C_{trap}$ and (b) $R_{ct,trap}$ among hematite samples decorated with different amount of surface cobalt cocatalyst loadings.

More piece of evidence regarding to the effect of surface $Co_3O_4$ distribution on water-splitting performance of hematite can be found by using the method of electronic impedance spectroscopy. The simplified equivalent circuit adopted herein was to emphasize the role of surface states stemming from the surface $Co_3O_4$ as shown in Figure S5. This equivalent circuit contains a charge transfer resistance ($R_{ct,trap}$) and a capacitance ($C_{trap}$) of trapping states, which is suggested to be a good approximation for the charge transfer from the surface trap state of surface $Co_3O_4$ to water molecules.[30] Figure S5 shows the representative EIS spectra collected under illumination with an applied potential of 0.4 V vs SCE. The nice fitting curves suggest that the adopted equivalent circuit can be applied to describe the surface states of these cobalt decorated hematite samples. When plotting as-determined $C_{trap}$ against applied potential under illumination (Figure 4a), it was noted that the charging of the surface state consistently shifted towards lower applied potential as increasing surface $Co_3O_4$ loadings. This could be attributed to the formation of a Schottky-type hetero-junction at the hematite/cobalt oxide/electrolyte interfaces.[13] Although the charging of surface states was obvious, we did not observe a concurrent decrease in $R_{ct}$, as noted in literature[24] (Figure 4b). A possible explanation is that the huge charge transport resistance in hematite/FTO interfaces overwhelms the reduction of $R_{ct}$, as these hematite electrodes were prepared through the dipping-annealing method. In this case, the resistance at hematite/FTO interface was found to be in a level approximately several megaohm.[31] We are currently working on associating $Co_3O_4$ to hydrothermally grown hematite electrodes and the results will be submitted separately.

#### Conclusions

By adopting the knowledge of surface complexation modeling, we have demonstrated in this study the preparation of homogeneously distributed $Co_3O_4$ on hematite surfaces. Also, the mechanism behind these preparation processes has addressed from the point of view of aqueous and surface chemistry. First, a neutral or an alkaline environment is very important for the surface hydroxyl groups of hematite to deprotonate and then stoichiometrically accommodate $Co^{2+}$. The concentration of the initial $Co^{2+}$ is another important parameter as a high $Co^{2+}$ concentration could result in the precipitation of $Co(OH)_2$, which would be converted to coarse $Co_3O_4$ in the end of thermal treatment. Different surface distributions of $Co_3O_4$ directly affect the efficiency of water oxidation reactions and photodegradation of organic dyes. Finally, our results successfully bridged the knowledge between environmental sciences and material chemistry.

## Acknowledgements

We thank National Science Council, Taiwan (NSC102-2113-M-007-003-MY2) for supporting this study. The authors greatly appreciate the access of facilities at CNMM of NTHU. WW is grateful for the financial support from National Natural Science Foundation of China (Grant No. 11402069) and Shenzhen Peacock Technological Innovation Program (Grant No. KQCX20140521144102503).

## Notes and references

[a] Biomedical Engineering and Environment Sciences, National Tsing Hua University, Hsinchu, Taiwan; [b] School of Material Sciences and Engineering, Harbin Institute of Technology, Shenzhen Graduate School, Shenzhen, PR China; [c] Department of Chemical Engineering, National Tsing Hua University, Hsinchu, Taiwan; d Institute of Urban Environment, Chinese Academy of Science, Xiamen, China
† Corresponding Author : thwang@mx.nthu.edu.tw; cfwang@mx.nthu.edu.tw

Electronic Supplementary Information (ESI) available: [Supporting information addressing the amount of surface cobalt loadings (Table S1) and Figures S1- S5 are available free of charge via the Internet]. See DOI: 10.1039/b000000x/

1 J. Lin, AQ. Wang, BT. Qiao, XY. Liu, XF. Yang, XD. Wang, JX. Liang, J. Li, JY. Liu, T. Zhang, *J. Am. Chem. Soc.*, **2013**, 135,15314–15317.
2 J. Thomas, Z. Saghi, P. Gai, P. *Top. Catal*. **2011**, 54, 588-594.
3 X. Yang, A. Wang, B. Qiao, J. Li. J. Liu, T. Zhang, *Acc. Chem. Res*. **2013**, 46, 1740-1748.
4 F. Schuth, Angew. *Chem. Int. Ed*. **2014**, 53, 8599-8604.
5 TH. Wang, CJ. Hsieh, SM. Lin, DC. Wu, MH. Li, SP. Teng, *Environ. Sci. Technol*. **2010**, 44, 5142-5147.
6 C. Tiberg, C. Sjostedt, I. Persson, J.P. Gustafsson, *Geochim. Cosmochim. Acta* **2013**, 120, 140-157.
7 M. Gunnarsson, A-M. Jakobsson, S. Ekberg, Y. Albinsson, E. Ahlberg, *J. Colloid Interf. Sci*. **2000**, 231, 326-336.
8 WD. Schecher, DC. McAvoy, MINEQL+: A chemical equilibrium modeling system, version 4.5 for Windows, User's manual, v2.00; Environmental Research Software: Hallowell, Maine, 2003.
9 DA. Dzombak, F.M.M. Morel, Surface complexation modeling: Hydrous Ferric Oxide, Wiley-Interscience, New York, 1990.
10 LF. Xi, PD. Tran, SY. Chiam, P.S. Bassi, W.F. Mak, H.K. Mulmudi, S.K. Batabyal, J. Barber, JSC. Loo, LH. Wong, L.H. *J. Phys. Chem. C* **2012**, 116, 13884−13889.
11 R. Suresh, R. Prabu, A. Vijayaraj, K. Giribabu, A. Stephen, V. Narayanan, *Mater. Chem. Phys*. **2013**, 134, 590-596.
12 T.P. Almeida, M.W. Fay, YQ. Zhu, P.D. Brown, *J Mater Sci* **2012**, 47, 5546–5560.
13 M. Barroso, A.J. Cowan, S.R. Pendlebury, M. Gratzel, D.R. Klug, J.R. Durrant, *J. Am. Chem. Soc*. **2011**, 133, 14868–14871.
14 S.C. Riha, B.M. Klahr, E.C. Tyo, S. Seifert, S. Vajda, M.J. Pellin, T.W. Hamann, A.B.F. Martinson, *ACS Nano*, **2013**, 7, 2396–2405.
15 M.W. Kanan, D.G. Nocera, *Science*, **2008**, 321, 1072-1075.
16 D.K. Zhong, JW. Sun, H. Inumaru, D.R. Gamelin, *J. Am. Chem. Soc*. **2009**, 131, 6086–6087.
17 M. Barroso, C.A. Mesa, S.R. Pendlebury, A.J. Cowan, T. Hisatomi, K. Sivula, M. Grätzel, D.R. Klug, J.R. Durrant, *Proc. Natl. Acad. Sci. USA*, **2012**, 25, 15640–15645.
18 K.J. McDonald, KS. Choi, *Chem. Mater*. **2011**, 23, 1686–1693.
19 R. Franking, LS. Li, M.A. Lukowski, F. Meng, YZ. Tan, R.J. Hamers, S. Jin, *Energy Environ. Sci*. **2013**, 6, 500–512.
20 V. Barron, J. Torrent, *J. Colloid Interf. Sci*. **1996**, 177, 407–410.
21 C.L. Peacock, D.M. Sherman, *Geochim. Cosmochim. Acta*, **2004**, 68, 2623–2637.
22 WR. Zhao, JL. Gu, LX. Zhang, HG. Chen, LJ. Shi, *J. Am. Chem. Soc*. **2005**, 127, 8916-8917.
23 I. Kobal, P. Hesleitner, E. Matijevic, *Colloids and Surfaces*, **1988**, 33, 167-174.

24 B. Klhar, S. Gimenez, F. Fabregat-Santiago, T. Hamann, H. Bisquert, *J. Am. Chem. Soc*. **2012**, 134, 4294-4302.
25 JJ. Deng, XX. Lv, J. Gao, A.W. Pu, M. Li, XH. Sun, J. Zhong, *Energy Environ. Sci*. **2013**, 6, 1965-1970.
26 S. Ardizzon, G. Spinolo, S. Trasatti, S. Electrochim. Acta 1995, 40, 2683-2686.
27 L. Vayssieres, N. Beermann, S.-E. Lindquist, A. Hagfeldt, *Chem. Mater*. **2001**, 13, 233–235.
28 XM. Zhou, HC. Yang, CX. Wang, XB. Mao, YS. Wang, YL. Yang, G. Liu, *J. Phys. Chem. C* **2010**, 114, 17051–17061.
29 KQ. Wu, YD. Xie, JC. Zhao, HS. Hidaka, *J. Molecular Catalysis A: Chem*. **1999**, 144, 77–84.
30 B. Klahr, S. Gimenez, F. Fabregat-Santiago, J. Bisquert, T.W. Hamann, *J. Am. Chem. Soc*. **2012**, 134, 16693−16700.
31 TH. Wang, MC. Huang, FW. Liu, YK. Hsieh, WS. Chang, JC. Lin, CF. Wang, *RSC Advances*, **2014**, 4, 4463-4471

## Graphic Abstract